AMERICAN SCIENTIFIC PUBLISHERS

Journal of Medical Imaging and Health Informatics
Vol. 9, 175–182, 2019

A Novel Medical Image Edge Detection Method Based on Reinforcement Learning and Ant Colony Optimization

Xinhua Wang[1,2], Jihong Ouyang[1,*], Yungang Zhu[1], Haibo Yu[3], and Helong Li[3]

[1]*College of Computer Science and Technology, Key Laboratory of Symbolic Computation and Knowledge Engineering of Ministry of Education, Jilin University, Changchun 130012, China*
[2]*State Key Laboratory of Applied Optics, Changchun Institute of Optics, Fine Mechanics and Physics, Chinese Academy of Sciences, Changchun 130012, China*
[3]*China Electric Power Research Institute, Beijing 100192, P. R. China*

Edge detection is one of the most essential steps and research focuses in medical imaging. In recent years, ant colony optimization has been widely used in medical image edge detection due to its robustness and accuracy. To further improve the performance of ant colony optimization based medical image edge detection methods, in this paper we proposed a novel strategy combining ant colony optimization and machine learning. At first, instead of using a constant number of neighborhood pixels to calculate the heuristic information for each pixel, we integrate multi-agent reinforcement learning into the movement of artificial ants to select variable perceived radius to calculate heuristic information. Additionally, another adaptive parameter is presented to control the moving direction of artificial ants in order for jumping from local optima. The proposed method is evaluated on typical medical images, and the experimental results show that the proposed method can perform high-precision edge detection for medical images.

Keywords: Medical Imaging, Image Processing, Ant Colony Optimization, Reinforcement Learning.

1. INTRODUCTION

Nowadays, increasing image data are used in medical area. Medical Image edge detection aims at identifying a set of connected curves that indicate the boundaries of significant objects in medical digital image.[1] By detecting edge of a medical image, one could extract useful medical information, such as volume, shape and motion of organs, from MRI, CT, X-ray, thermal, etc., which helps to detect abnormalities of patients.[2] Therefore, image edge detection is one of the most crucial steps in medical imaging.

Medical images are often multi-level imaging involving human tissue. The automated edge detection of medical images is difficult due to imaging deficiencies such as noise, artifacts, and partial volume effects. Compared with ordinary images, the composition of medical images is often complicated, and the variation of the gray intensity value is also complicated. Furthermore, the medical images always suffer from noise such as Gaussian noise.[3] The traditional numerical differential-based methods usually adopted local information of a pixel to determine the edge, and are sensitive to noise. These restrict their performance for medical image edge detection. Therefore, in recent years the ant colony optimization (ACO) has received more and more attention in the field of medical edge detection due to its robust optimization and global search ability. However, most ACO-based edge detection methods confront crucial weaknesses restricting the accuracy of the detection. Existing methods adopted a fixed number of neighborhood pixels, which we called fixed perceived radius, to calculate the gradient in the heuristic information for each pixel in transition probability. That leads to some pixels in the edge may not be detected or some pixels not belong to image edge are detected. In other words, lose some important edges or detect worthless edges. In addition, the movement of artificial ants tends to converge prematurely, result in obtaining local optima instead of global optima, especially for the large image.

To address above issues, in this paper we propose a novel strategy for medical image edge detection which combining ant colony optimization and machine learning technique. Instead of using fixed and constant number of neighborhood pixels to compute the gradient, we integrate multi-agent reinforcement learning in the movement of artificial ants to determine variable number of neighborhood pixels for each pixel according to the surrounding scenarios of the pixel adaptively. Another adaptive parameter

*Author to whom correspondence should be addressed.

is also introduced to control the direction of movement of artificial ants to prevent local optima. The proposed method is more suitable for the complicated multi-level medical image and complicated variation of the gray intensity, and is immune to noise.

The remainder of this paper is organized as follows: Section 2 offers brief background knowledge concerning about ant colony optimization. Section 3 presents the related works of this article. The proposed method is described in detail in Section 4. The experimental results and analysis are presented in Section 5. Finally, conclusions and recommendations for future works are summarized in Section 6.

2. PRELIMINARIES OF ANT COLONY OPTIMIZATION

The original ant colony optimization (ACO) algorithm was proposed by Dorigo and is one of the most well-known bio-inspired algorithms that can be applied to a wide range of optimization problems.[4] The ACO algorithm is inspired by the natural phenomenon that while searching for food, ants deposit pheromones on the route they travel, and their colony mates can detect the pheromones to guide their route. Therefore, ants search for food on the route that follows the maximum intensity of pheromones. ACO is a probabilistic technique that detects optima in a graph using a guided search, and has been widely applied in many fields.

During the initialization process of the ACO algorithm, a predefined number of artificial ants were put on the search space. In the construction process, the ants move through the search space and deposited pheromones on the route they traveled. The movement of each ant is according to a transition probability, which indicate the probability with which an ant moves from one unit to another unit in the search space. The value of the transition probability is dependent on the pheromones and heuristic information of the unit. After the ants move, the pheromones are updated. The search terminates when a predefined number of iterations is reached. Then, the optimal solution is chosen as the route that the most ants traveled and subsequently contained more pheromones.

3. RELATED WORKS

Due to the disadvantages of traditional edge detection methods, ACO, as a meta-heuristic approach, has recently been used to solve image edge detection problems. And based on ACO, several different techniques have also been proposed.

Nezamabadi et al. used eight neighborhood pixels to compute the gradient of each pixel in the heuristic function of the ant system, and derived the relationship between image size and the number of artificial ants.[5] Tian et al. adopted the ant colony system and proposed a novel local structure containing sixteen pixels around each pixel; this structure was then used to compute the gradient of each pixel.[6] In Liu's method, a local structure of 24 pixels was employed to compute the gradient in the heuristic function of ACO to realize convenient image edge detection; a group of empirical values for the algorithm was also proposed.[7] Etemad et al. defined two types of pheromones, the first of which indicates the features to be extracted, and the second was defined by the Euclidean norm of the image gradient.[8] Lu et al. studied the ACO algorithm to compensate broken edges, and adopted four moving policies to reduce the computational load.[9] Rezaee et al. introduced an energy state in the transition probability for each ant in order to enhance efficiency.[10] Chen et al. adopted particle swarm optimization to enhance parameters in an ACO-based edge detection method, and designed a fitness function based on connectivity of image edges to evaluate the quality of parameters in ACO.[11]

Mullen et al. introduced an adaptive thresholding method to ACO-based image edge detection, which enabled automated distributed adaptive thresholding and eliminated the need for user-defined thresholds.[12] Huan gets image edge according to different neighborhood access policy, and use the best neighborhood strategy to get detection. Compared with the traditional edge detection methods, the algorithm can effectively suppress the noise interference.[13] Ari et al. presented a novel method that combined ant colony optimization with the Fisher ratio. In this method, the Fisher ratio was utilized to determine the optimum threshold value for updating the pheromone matrix.[14] Gopalakrishnan et al. applied the ACO algorithm for lung nodule detection, which involved refined ACO, logical ACO, and variant ACO; in addition, they proposed a black circular neighborhood approach to detect nodule centers from the edge detected image.[15] Koner et al. presented eight variations in the implementation of ACO-based edge detection by modifying initialization and construction phases.[16] Ashir et al. first decomposed images by dual-tree complex wavelet transform to obtain the oriented wavelets and approximation versions of the original image and then applied ACO to each of the decomposed images.[17]

As mentioned previously, most existing ACO-based methods do not use varying numbers of neighborhood pixels to compute the gradient of each pixel based on the content around it; they also tend to suffer from premature convergence, particularly in large images. These drawbacks were the motivation for this study.

4. THE PROPOSED METHODOLOGY

In the image edge detection method based on ant colony optimization, the image with $M \times N$ pixels is mapped as a 2-dimensional $M \times N$ grids, each pixel of the image corresponds to a cell of the 2-dimensional grid. A pheromone matrix is constructed by the movement of a number of artificial ants on the image grid, and then the edge is detected based on the pheromone matrix.

n artificial ants are put on the n cells in the two-dimensional image grid (corresponds to n pixels of the image) initially. Then for each ant, it moves from one pixel to another pixel according to the transition probability, and deposits pheromone on the pixel it visited. This procedure is repeated until convergence or reaching a threshold times. Then the pixels with higher pheromone are more probable to belong to the edges of the image.

4.1. Initialization

For the initialization of the algorithm, a predefined number of ants are put in the pixels of the $M \times N$ image. The initial values of the pheromone are set to a random value.

4.2. Novel Transition Probability

In each step of iteration, each artificial ant moves from current pixel to another pixel of the image according to a transition

probability. The proposed transition probability for ant moving from pixel (r, s) to pixel (x, y) is as follows:

$$P_{(r,s)\to(x,y,k)} = \begin{cases} \dfrac{(\tau_{(x,y)})^{\alpha}(\psi_{(x,y,k)})^{\beta}(\theta_{(x,y)})^{\gamma}}{\sum_{\substack{(x,y)\\ \in\Omega(r,s)}} (\tau_{(x,y)})^{\alpha}(\psi_{(x,y,k)})^{\beta}(\theta_{(x,y)})^{\gamma}}, & \text{if } (x,y)\in\Omega(r,s) \\ 0, & \text{otherwise} \end{cases} \quad (1)$$

where $\tau_{(x,y)}$ is pheromone and $\psi_{(x,y,k)}$ is heuristic information for pixel (x, y). $\Omega(r, s)$ is a set that includes the neighborhood of pixel (r, s). α is the influence factor for $\tau_{(x,y)}$ and β is the influence factor for $\psi_{(x,y,k)}$. $\theta_{(x,y)}$ and γ will be explained later.

The heuristic information ψ guides the tendency of movement of artificial ant. Heuristic information of pixel (x, y) is usually designed as the "gradient" of the image intensity value at pixel (x, y), and parameter k represents the perceived radius for computing the gradient of pixel (x, y). ψ is defined as formula (2):

$$\psi_{(x,y,k)} = P(k \mid (r,s), a_{(r,s)\to(x,y)}) \cdot \frac{\ln \operatorname{grad}_k I_{x,y}}{\sum_{i=1}^{M}\sum_{j=1}^{N} \ln \operatorname{grad}_k I_{x,y}} \quad (2)$$

where

$$\operatorname{grad}_1 I_{x,y} = |I_{x-1,y-1} - I_{x+1,y+1}| + |I_{x-1,y} - I_{x+1,y}| + |I_{x-1,y+1} - I_{x+1,y-1}| + |I_{x,y-1} - I_{x,y+1}|$$

and

$$\begin{aligned} \operatorname{grad}_2 I_{x,y} = {} & |I_{x-2,y-1} - I_{x+2,y+1}| + |I_{x-2,y+1} - I_{x+2,y-1}| \\ & + |I_{x-1,y-2} - I_{x+1,y+2}| + |I_{x-1,y-1} - I_{x+1,y+1}| \\ & + |I_{x-1,y} - I_{x+1,y}| + |I_{x-1,y+1} - I_{x+1,y-1}| \\ & + |I_{x-1,y+2} - I_{x+1,y-2}| + |I_{x,y-1} - I_{x,y+1}| \end{aligned}$$

$I_{x,y}$ is the image intensity value of pixel (x, y). $\operatorname{grad}_1 I_{x,y}$ is to compute the "gradient" of the image intensity value at pixel (x, y) using 8 adjacent pixels of (x, y), and this strategy is considered as "perceived radius of 1." $\operatorname{grad}_2 I_{x,y}$ considers the 16 adjacent pixels as the neighborhood of pixel (x, y) to compute the gradient, and this strategy is regarded as "perceived radius of 2."

As mentioned before, the proposed method adopts variable perceived radius to compute the gradient of each pixel, in other words, uses different perceived radius for different pixels. This strategy can adaptively adopt different information according to the scenario of a pixel of the medical image and has potential to reduce noise, so it is more suitable for the complicated medical images.

The perceived radius for each pixel is selected with probability adaptively by reinforcement learning. Reinforcement learning is an area of machine learning inspired by behaviourist psychology, concerned with how software agents ought to take actions in an environment so as to maximize some notion of cumulative reward. In the proposed reinforcement learning strategy, the state of the ant is its location in the 2-dimensional $M \times N$ image grid, i.e., State $= (r, s)$. The action of ant is a pair Action $= (a, k)$, which means the action includes two sub-action, the first one a is the movement from its current location to its adjacent location in the image grid. The second sub-action k is the perceived radius. After the ant selects an action at a state, it will get a reward. The Q(State, Action) function, i.e., $Q((r, s), a, k)$ is the maximum reward ant can achieve by using the movement a and selecting perceived radius k as the first action from state (r, s). The value Q function is set to random positive value initially, and updated as follows after each artificial ant moves:

$$Q(\text{State, Action}) = Q((r,s),a,k) \leftarrow \text{reward} + \gamma \max_{a',k'} Q((r,s)', a', k') \quad (3)$$

where $(r, s)'$ is the next state of (r, s) after taking action (a, k). All the ants share the Q function and maintain the Q function concurrently.

During the movement of artificial ants, the perceived radius is decided by $P(k \mid (r, s), a)$, this probability can be calculated as follows:

$$P(k \mid (r,s), a) = \frac{P((r,s),a,k)}{P((r,s),a)} \propto P((r,s),a,k) \quad (4)$$

In formula (6), denominator does not contain k, so the formula is in proportion to numerator.

$$P((r,s),a,k) = \frac{Q((r,s),a,k)}{\sum_{a,k} Q((r,s),a,k)} \quad (5)$$

From formula (5) shows that the perceived radius selection probability $P(k \mid (r, s), a_{(r,s)\to(x,y)})$ in formula (2) can be obtained by Q function:

$$P(k \mid (r,s), a_{(r,s)\to(x,y)}) \propto Q((r,s), a_{(r,s)\to(x,y)}, k) \quad (6)$$

In formula (1), $\theta_{(x,y)}$ is the orientation factor to control the direction of the ants' movement, and γ is the influence factor for the orientation factor. $\theta_{(x,y)}$ can be defined as follows:

$$\theta_{(x,y)} = \begin{cases} \dfrac{1}{|r_{\text{pre}} + x - 2r| + |s_{\text{pre}} + y - 2s| + \varepsilon} & \text{step} < \text{threshold} \\ 1 & \text{otherwise} \end{cases} \quad (7)$$

where (r, s) is the current location of the ant, $(r_{\text{pre}}, s_{\text{pre}})$ is the previous step location of the ant, and (x, y) is the next location of the ant. ε is an extremely small constant to avoid the denominator equaling 0.

Figure 1 shows two examples to explain the first equation of $\theta_{(x,y)}$. As previously described, (r, s) is the current location of the ant, $(r_{\text{pre}}, s_{\text{pre}})$ is the previous location of the ant, and the grey cells of the structure are the possible locations the ant will go; the numbers in the cells show the value of $|r_{\text{pre}} + x - 2r| + |s_{\text{pre}} + x - 2s|$. Therefore, if the ant moves in a similar direction as before, $\theta_{(x,y)}$ is larger; otherwise, if the ant deviates from its original direction, $\theta_{(x,y)}$ is smaller.

Formula (1) and (7) guarantee that in the initial phase and middle phase of the search, the ants move in the same direction as far as possible, and do not go backwards. This allows the algorithm to achieve the optimal solution quickly. Then in the end phase, the ants can move in any direction, which helps the search jump out the local optima. This strategy enables the algorithm

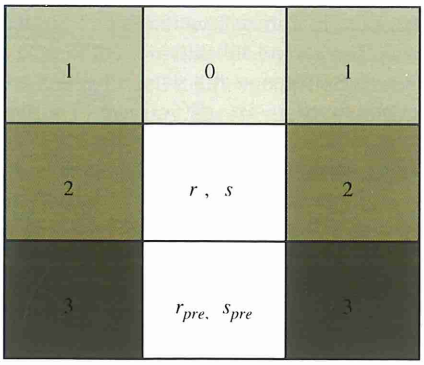

(a) Move from bottom to up

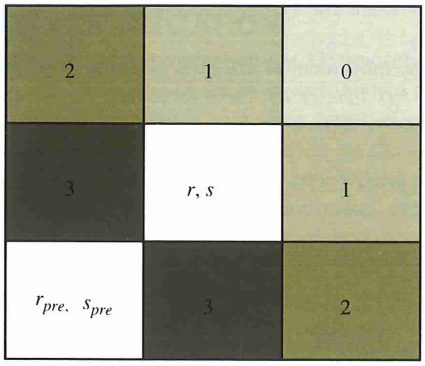

(b) Move from bottom-left to up-right

Fig. 1. Examples to explain formula 7.

to perform more global search than deterministic methods, and adapts to the complicated medical images.

The proposed method can be used for medical images with any pixel resolution. The higher pixel resolution is, the more running time the algorithm will take. Mao proposed another method[18] with variable perceived radius, but their method uses ACO to search perceived radius, which enlarging the search space of ACO, and their method do not use orientation factor.

4.3. Pheromone Updating and Edge Detection

At n-th iteration of the algorithm, after each ant moves one step, the ant updates the pheromone on the pixel (x, y) it visited by:

$$\tau_{(x,y)} = (1-\rho)\tau_{(x,y)} + \rho \sum_{k} \psi_{(x,y,k)} \tag{8}$$

where ρ is an evaporation coefficient.

The reward of ant after it moves to pixel (x, y) is defined as the difference between pheromone of pixel (x, y) and its adjacent pixels:

$$\text{reward} = \sum_{u,v=-1,0,1} (\tau_{(i,j)} - \tau_{(i+u,j+v)}) \tag{9}$$

Then the Q function is updated by formula (3). After all the ants move one step, the pheromone matrix is updated by:

$$\tau = (1-\varphi)\tau + \varphi\tau^0 \tag{10}$$

where φ is an attenuation coefficient of pheromone, τ^0 is the initial pheromone matrix.

ρ and φ are used to avoid the ant deposit profuse pheromone in a route, so as to avoid local optima.

The search terminates when the threshold number of iterations is reached, then the final pheromone matrix can be used to detect the edges in the image.

An intensity threshold is calculated based on Ref. [18]: firstly, selecting the average value T in the pheromone matrix, and using T as the initial value of the threshold. Secondly, dividing the pheromone matrix into two groups, one includes the elements larger than T, and the other group contains the elements less than T. Thirdly, computing the average values of the two groups separately, i.e., T_1, T_2, then let $T = (T_1 + T_2)/2$. Repeat above three steps until T is not changed, then we obtain T as the threshold, if the value of element in pheromone matrix is larger than T, then the corresponding pixel belongs to edge, otherwise the pixel is not belong to edge.

4.4. Overall Framework of the Algorithm

Therefore, the proposed algorithm is described as follows:

ALGORITHM (MEDICAL IMAGE EDGE DETECTION BASED ON ACO AND REINFORCEMENT LEARNING).

Input: an medical image with $M \times N$ pixels
Output: binary image with edges;
Put n ants on the pixel grid of the image;
Initialize the pheromone matrix τ and Q function;
for $i = 1$ **to** threshold_iteration_num **do**
  for each *ant* **in** ant colony **do**
    (r, s) = current location of *ant*
    for each $(x, y) \in \Omega(r, s)$ **do**
      Compute $\theta_{(x,y)}$ by Formula (7)
      for $k = 1$ **to** 2 **do**
        Compute perceived radius selection probability $P(k \mid (r, s), a)$ by Formula (6);
        Compute heuristic information $\psi(x, y, k)$ by Formula (2);
        Compute transition probability $P_{(r,s)\to(x,y,k)}$ by Formula (1);
      end for
    end for
    Select x, y, k based on probability $P_{(r,s)\to(x,y,k)}$;
    ant move to pixel (x, y);
    Update $\tau_{(x,y)}$ by Formula (8);
    Compute reward by Formula (9);
    Update $Q((r, s), a_{(r,s)\to(x,y,k)}, k)$ function by Formula (3);
  end for
  Update τ by Formula (10);
end for
Generate intensity threshold T based on τ;
Detect edge pixels of the image using T.

5. EXPERIMENTAL RESULTS AND ANALYSIS

In this section, we select some typical medical images to measure the proposed method by comparing with other similar state of the art methods. All the experiments are performed on a PC with 64-bit Intel Core i7 3.5 GHz CPU and a RAM of 16 GB, the code is written by MATLAB R2011b. The main parameters of the proposed are set as follows: the number of ants is $\sqrt{M \cdot N}^5$ for an $M \times N$ pixels image, pheromone influence factor $\alpha = 6$, heuristic information influence factor $\beta = 0.1$, orientation influence factor

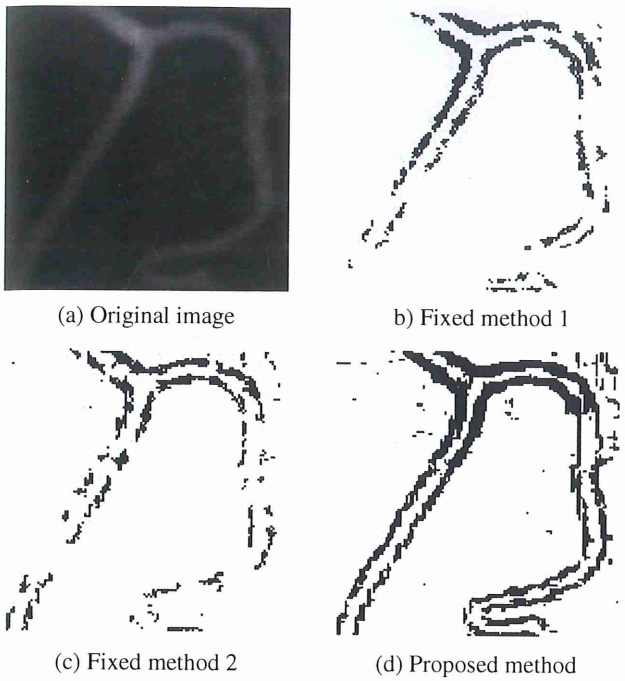

(a) Original image b) Fixed method 1

(c) Fixed method 2 (d) Proposed method

Fig. 2. Edge detection results for an X-ray image of blood vessel.

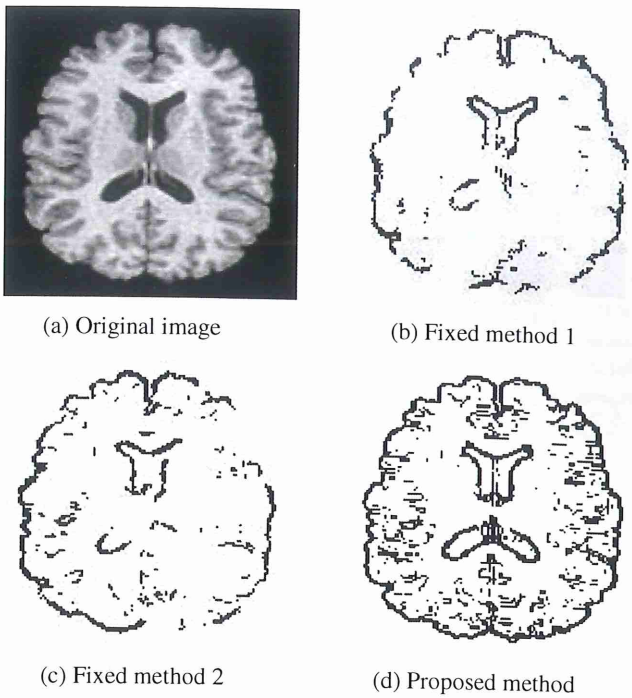

(a) Original image (b) Fixed method 1

(c) Fixed method 2 (d) Proposed method

Fig. 4. Edge detection results for a magnetic resonance image for brain.

$\gamma = 1$, the initial pheromone $\tau^0 = 0.0001$, the maximum iteration number is 1000.

We select several typical medical images[19–24] to evaluate the proposed method. There are two X-ray images of blood vessel (Figs. 2 and 3), a magnetic resonance image for brain (brain MRI) (Fig. 4), a foot X-ray image with low contrast (Fig. 5), and some cells image (Fig. 6), and three complex medical images: two nuclear body skeleton scans (Figs. 7–8) and a cell image with Gaussian noise (mean value is 0 and variance is 0.02) (Fig. 9).

We compare the proposed method with two other typical state of the art methods. One is an ACO-based method in Ref. [5], this method uses a fixed perceived radius of 1 to compute the gradient in heuristic information and do not use the orientation factor, we called this method "Fixed Method 1" for short. Another is

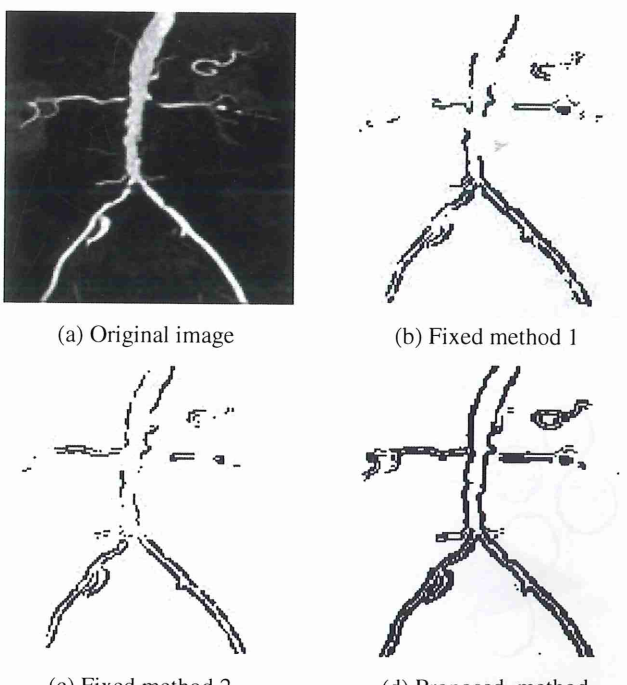

(a) Original image (b) Fixed method 1

(c) Fixed method 2 (d) Proposed method

Fig. 3. Edge detection results for another X-ray image of blood vessel.

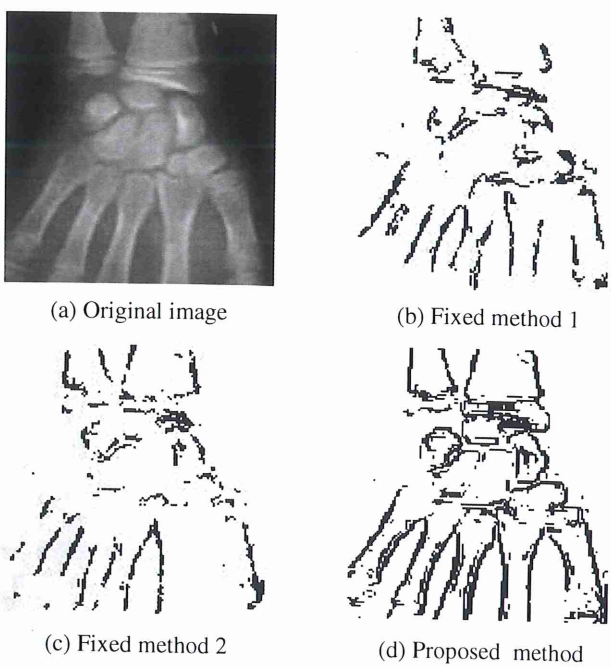

(a) Original image (b) Fixed method 1

(c) Fixed method 2 (d) Proposed method

Fig. 5. Edge detection results for a foot X-ray image.

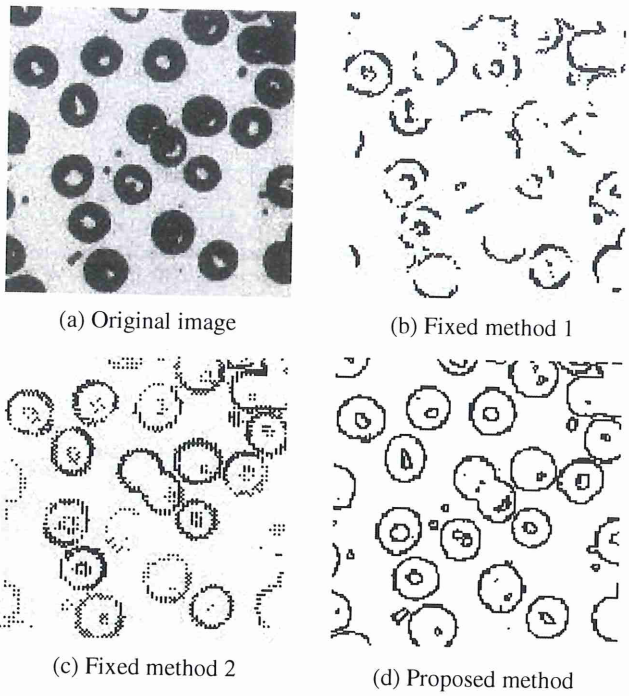

(a) Original image (b) Fixed method 1

(c) Fixed method 2 (d) Proposed method

Fig. 6. Edge detection results for cells image.

an ACO-based method in Ref. [6] with a fixed perceived radius of 2, we called this method "Fixed Method 2" for short. For each test image, we provide the edge detective results of the proposed method and other two compared methods. In detail, Figures 4 to 10 show the test results, in each figure, subfigure (a) presents the original image, and subfigure (b) shows the edge detective result of Fixed method 1, subfigure (c) shows the results of Fixed method 2, and subfigure (d) shows the result of our proposed method.

It can be observed from Figures 2 to 8 that the proposed method can detect more edge pixels which are not obvious.

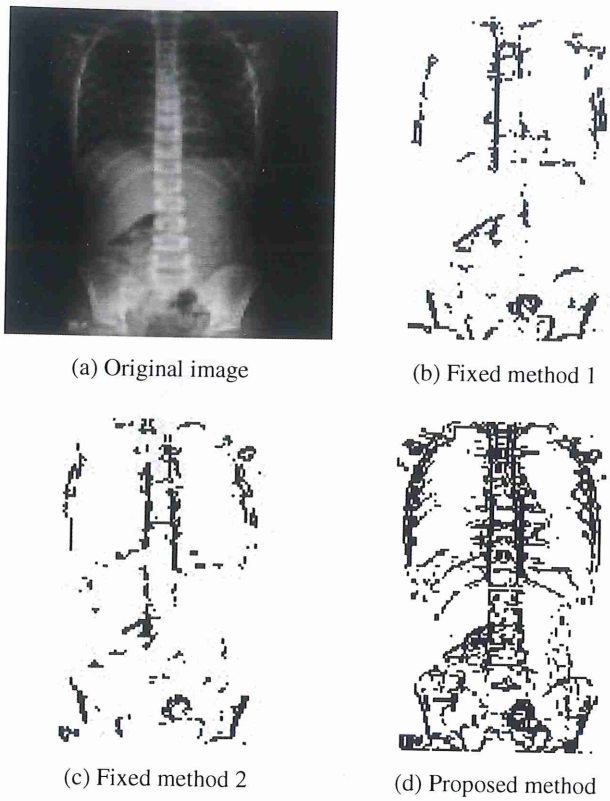

(a) Original image (b) Fixed method 1

(c) Fixed method 2 (d) Proposed method

Fig. 8. Edge detection results for a nuclear body skeleton scan.

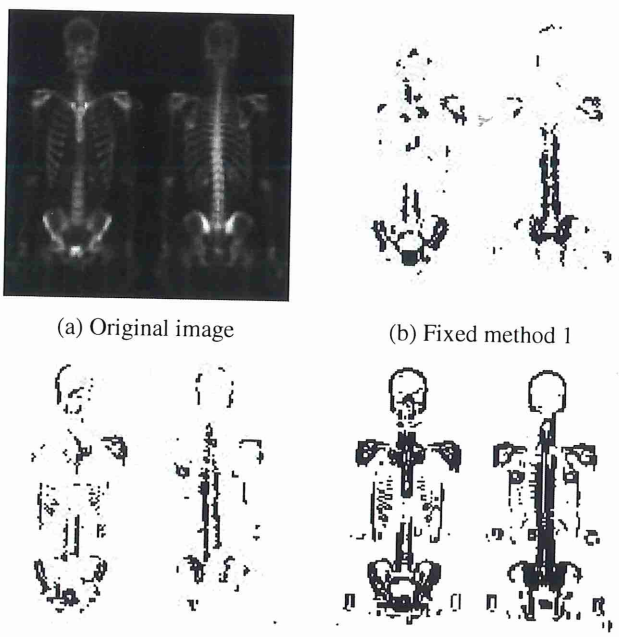

(a) Original image (b) Fixed method 1

(c) Fixed method 2 (d) Proposed method

Fig. 7. Edge detection results for a nuclear whole body skeleton scan.

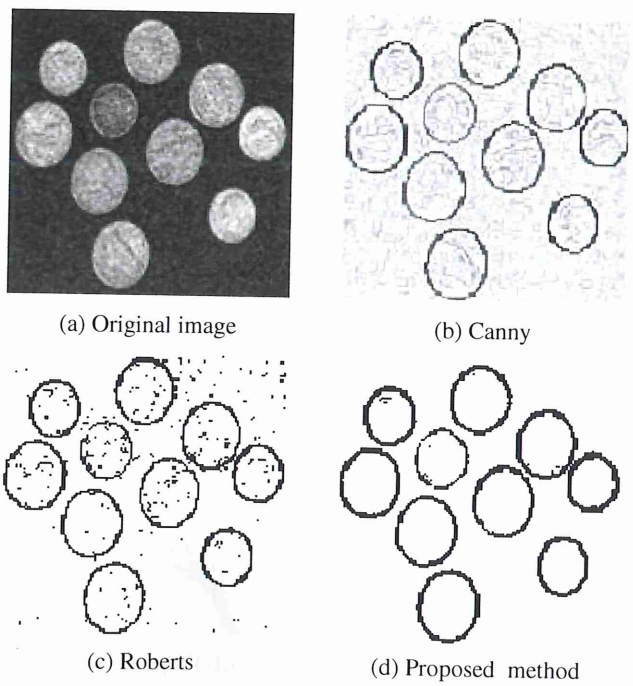

(a) Original image (b) Canny

(c) Roberts (d) Proposed method

Fig. 9. Edge detection results for a noisy cell image.

Table I. Quantitative comparison results of the methods.

	Fixed method 1	Fixed method 2	Proposed
Completeness	0.77	0.86	0.93
Discriminability	12.83	16.62	19.71
Precision	0.73	0.85	0.89
Robustness	78.48	80.97	81.74

Figure 9 shows the result of the Canny and Roberts methods (two classical deterministic methods), we can also observe that the proposed method is more robust for the image with Gaussian noise than traditional deterministic methods. Therefore, the proposed method outperforms the competitors both in details and entirety.

We then adopt quantitative criteria proposed in Ref. [24] to evaluate the methods quantitatively. The criteria include Completeness, Discriminability, Precision and Robustness. Completeness is referred to as the ability of an edge detector to mark all possible edges of noiseless images. Discriminability is referred to as the ability of an edge detector to discriminate important from not important edges. Precision measures the ability of an edge detector to mark edges as close as possible from actual edges. Robustness measures the ability of an edge detector to be immune to noise.[25] We compare the proposed method with Fixed method 1 and 2. Table I shows the average value of the quantitative criteria of the methods on all the test images.

It can be observed from Table I that the proposed method the quantitative indicators of the proposed method are better than the competitors.

Figure 10 shows the pheromones deposited on the pixels of an image after the proposed algorithm terminated. The plane in the two horizontal axes indicates the image, and the vertical axis indicates the pheromones on each pixel. It is clearly illustrated that the proposed algorithm extracted edges in an efficient way, and that the pheromones are deposited on the edge pixels of the image correctly, meaning the proposed algorithm is effective.

The proposed method belongs to the empirical methods those are data-dependent, and so we make a primary sensitivity analysis. We change the value of the input variables or parameters in turn, and record the maximum and minimum of each above four quantitative criteria of the result image. Then we compute the ratio of the difference of maximum and minimum of each quantitative indicator to the maximum, and take average ratio for the four quantitative criteria. We observed that the perceived radius is most relevant to the results, so it is the reason for the strategy we proposed. The other parameters those has impact on the results are the maximum iteration number, pheromone influence factor, heuristic information influence factor, orientation influence factor successively.

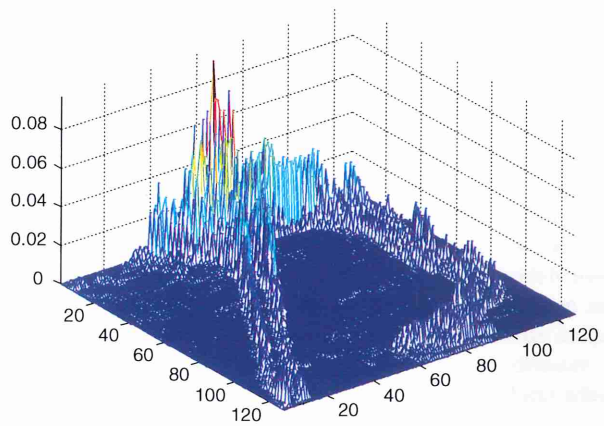

Fig. 10. Ultimate pheromone deposited on the images by artificial ants.

6. CONCLUSIONS AND FUTURE WORKS

To address the drawbacks of traditional ant colony optimization based medical edge detection methods, in this paper we proposed a novel method combining ant colony optimization and machine learning. Instead of using fixed perceived radius, we integrate multi-agent reinforcement learning in the movement of artificial ant to select variable perceived radius to calculate the gradient in heuristic information for each pixel. Another adaptive parameter is also presented to control the direction of movement of artificial ants to prevent premature convergence. The method is employed and evaluated on typical medical images, and the experimental results show that the proposed method performs high-precision edge detection for medical image. In future, we will design better reward for each action of artificial ant to further enhance the precision of perceived radius selection. We will also use other optimization algorithms such as grey wolf optimizer[26] and whale optimization,[27] other models such as Bayesian networks[28] and Evidence Theory[29] to detect the edge of complex medical image and perform more comprehensive sensitivity analysis for the method.

Acknowledgments: The authors would like to appreciate the handling editor and the anonymous reviewers, whose constructive and insightful comments greatly helped in improving this paper. This work was supported by the NSFC (61502198), Science and Technology Projects of State Grid, Science and Technology Development Program of Jilin Province of China (20160209006GX),

References and Notes

1. E U. Scott, Digital Image Processing and Analysis: Human and Computer Vision Applications with CVIP Tools, 2nd edn., CRC Press, Boca Raton **(2010)**.
2. X. Wang, Y. Zhu, J. Yang, L. Zhang, and C. Jiang, An efficient medical image segmentation approach based on modified evolutionary algorithm. *J. Med. Imaging Health Inf.* 5, 1563 **(2015)**.
3. S. C. Satapathy, K. S. Raju, J. K. Mandal, and V. Bhateja, Edge detection on an image using ant colony optimization, *2nd International Conference on Computer and Communication Technologies*, Hyderabad, India, July **(2015)**, pp. 593–599.
4. M. Dorigo, Optimization, Learning and Natural Algorithms, Ph.D. Dissertation, Politecnico Di Milano, Italy **(1992)**.
5. H. Nezamabadi, S. Saryazdi, and E. Rashedi, Edge detection using ant algorithms. *Soft Computing* 10, 623 **(2006)**.
6. J. Tian, W. Yu, and S.Xie, An ant colony optimization algorithm for image edge detection, *IEEE Congress on Evolutionary Computation*, Hong Kong, China **(2008)**, pp. 751–756.
7. X. Liu and S. Fang, A convenient and robust edge detection method based on ant colony optimization. *Optics Communications* 353, 47 **(2015)**.
8. S. A. Etemad and T. White, An ant-inspired algorithm for detection of image edge features. *Applied Soft Computing* 11, 4883 **(2011)**.
9. D. Lu and C. Chen, Edge detection improvement by ant colony optimization. *Pattern Recognition Letters* 29, 416 **(2008)**.
10. A. Rezaee, Extracting edge of images with ant colony. *Journal of Electrical Engineering* 59, 57 **(2008)**.
11. T. Chen, X. Sun, H. Han, and X. You, Image edge detection based on ACO and PSO algorithm. *International Journal of Advanced Computer Science and Applications* 6, 47 **(2015)**.
12. R. J. Mullen, D. N. Monekosso, and P. Remagnino, Ant algorithms for image feature extraction. *Expert Systems with Applications* 40, 4315 **(2013)**.

13. Y. Huan, Image edge detection based on ant colony optimization algorithm. *International Journal of Advanced Pervasive and Ubiquitous Computing* 8, 1 **(2016)**.
14. S. Ari, D. K. Ghosh, and P. K. Mohanty, Edge detection using ACO and F ratio. *Signal Image and Video Processing* 8, 625 **(2014)**.
15. R. C. Gopalakrishnan and V. Kuppusamy, Ant colony optimization approaches to clustering of lung nodules from CT images. *Computational and Mathematical Methods in Medicine* 2014, 1 **(2014)**, Article No. 572494.
16. S. Koner and S. Acharyya, Ant colony optimization variants in image edge detection, *3rd International Conference on Communications and Signal Processing*, Melmaruvathur, India, April **(2014)**.
17. A. M. Ashir and A. Eleyan, A multi-resolution approach for edge detection using ant colony optimization, *23rd Signal Processing and Communications Applications Conference*, Malatya, Turkey, May **(2015)**, pp. 1777–1780.
18. R. Mao, A swarm intelligence based medical image edge detection method with adaptive gradient. *J. Med. Imaging Health Inf.* 7, 1087 **(2017)**.
19. J. Wen, Z. Yan, and J. Jiang, Novel lattice boltzmann method based on integrated edge and region information for medical image segmentation. *Bio-Medical Materials and Engineering* 24, 1247 **(2014)**.
20. X. Shen, H. Pan, and H. Chen, Medical image segmentation algorithm based on one-dimensional otsu multiple threshold. *Journal of Jilin University (Science Edition)* 54, 344 **(2016)**.
21. D. L. Pham, C. Xu, and J. L. Prince, A Survey of Current Methods in Medical Image Segmentation, Technical Report, JHU/ECE 99-01 **(1999)**.
22. D. Shen, E. Xu, and L. Zhang, Application of improved sobel algorithm in medical image edge detection, *Applied Mechanics and Materials* 678, 151 **(2014)**.
23. A. S. Camp, M. Ruggeri, G. C. Munguba, M. L. Tapia, W. M. Simon, S. K. Bhattacharya, and R. K. Lee, Structural correlation between the nerve fiber layer and retinal ganglion cell loss in mice with targeted disruption of the Brn3b gene. *Investigative Ophthalmology and Visual Science* 52, 5226 **(2011)**.
24. X. W. Fu, M. Y. Ding, Y. G. Sun, and S. B. Chen, A new quantum edge detection algorithm for medical images. *Proceedings of the SPIE—The International Society for Optical Engineering* 7497, 1 **(2009)**.
25. R. Moreno, D. Puig, C. Julia, and M. A. Garcia, A new methodology for evaluation of edge detectors, *Proceedings of the 16th IEEE International Conference on Image Processing* **(2009)**, pp. 2157–2160.
26. S. Ozturk and B. Akdemir, Automatic leaf segmentation using grey wolf optimizer based neural network. *21st IEEE International Conference on Electronics, Palanga, Lithuania*, June **(2017)**, Vol. 2014, pp. 1–16.
27. S. Mirjalili and A. Lewis, The whale optimization algorithm. *Advances in Engineering Software* 95, 51 **(2016)**.
28. Y. G. Zhu, D. Y. Liu, Y. Li, and X. H. Wang, Selective and incremental fusion for fuzzy and uncertain data based on probabilistic graphical model. *Journal of Intelligent and Fuzzy Systems* 29, 2397 **(2015)**.
29. D. Y. Liu, Y. G. Zhu, N. Ni, and J. Liu, Ordered proposition fusion based on consistency and uncertainty measurements. *Science China Information Sciences* 60, 1, Article No.082103 **(2017)**.

Received: 21 June 2018. Revised/Accepted: 17 August 2018.